Discover Applied Sciences

RESEARCH Open Access

Numerical analysis of air layer effects on PCM melting in a horizontal double concentric tube

Karrar A. Hammoodi[1], Rassol Hamed Rasheed[2,3], Issa Omle[4*], Saif Ali Kadhim[5], Abdallah Bouabidi[6], Ravishankar Sathyamurthy[7,8], Mujtaba A. Flayyih[9], Abbas Fadhil Khalaf[10] and Farhan Lafta Rashid[11]

*Correspondence:
Issa Omle
issa.omle@uni-miskolc.hu

Full list of author information is available at the end of the article

Abstract

Latent heat thermal energy storage systems using phase change materials face key challenges, particularly the low thermal conductivity of phase change materials and the limited investigation of insulating effects like air layers within storage geometries. This study numerically examines the impact of air layers on the melting behavior of paraffin wax (RT42) inside a horizontal double concentric tube using a two-dimensional computational fluid dynamics model in ANSYS/FLUENT 16. Three configurations were analyzed: no air layer, a 1 mm air layer, and a 2 mm air layer surrounding the inner heated tube. The enthalpy-porosity method was applied to simulate the melting process, accounting for heat transfer by conduction and natural convection. Results show that introducing a 1 mm air gap extended the melting time by 28.57%, while a 2 mm air gap led to a 57.14% increase, primarily due to the added thermal resistance. This is the first study to quantitatively assess air layer effects in this geometry, offering new insights into optimizing phase change material-based storage systems by considering internal insulation phenomena.

Highlights

- Unintentional air pockets can greatly slow the heat storage process in energy systems by acting as an insulator.
- A small 2 mm air gap delays the full energy charging time of the horizontal double concentric tube by more than 50%.
- Designers must account for internal air gaps to prevent major performance losses in phase change material devices.

Keywords Double concentric tube, Shell-and-tube, PCM, Melting time, CFD

1 Introduction

Phase Change Materials (PCMs) have garnered increasing attention for use in passive Thermal Energy Storage (TES) systems that support renewable energy technologies such as solar and wind. These sources are inherently intermittent, necessitating efficient storage solutions that can balance supply and demand [1, 2]. PCMs are particularly suitable for TES due to their ability to absorb and release significant amounts of latent heat during phase transitions [3]. Applications of PCMs span across solar heating, building

© The Author(s) 2026. **Open Access** This article is licensed under a Creative Commons Attribution 4.0 International License, which permits use, sharing, adaptation, distribution and reproduction in any medium or format, as long as you give appropriate credit to the original author(s) and the source, provide a link to the Creative Commons licence, and indicate if changes were made. The images or other third party material in this article are included in the article's Creative Commons licence, unless indicated otherwise in a credit line to the material. If material is not included in the article's Creative Commons licence and your intended use is not permitted by statutory regulation or exceeds the permitted use, you will need to obtain permission directly from the copyright holder. To view a copy of this licence, visit http://creativecommons.org/licenses/by/4.0/.

energy management, and heat exchangers [4–6]. Despite their advantages—such as high latent heat, chemical stability, and low vapor pressure—PCMs suffer from low thermal conductivity, which limits heat transfer rates during melting and solidification [7, 8]. Numerous studies have attempted to overcome this limitation by enhancing thermal conductivity through the use of extended surfaces (fins), nanoparticles, or optimized geometric configurations [9–11]. Recent investigations have focused on fin design, metal foams, and hybrid additives to improve melting/solidification behavior in PCM-based systems [12, 13].

Basem et al. [14] investigated how fast PCM melts in a semi-cylindrical cell both with and without fins. Their findings demonstrated that adding fins to the cell significantly increases the PCM melting rate. Comparing cells with three and five fins to those without, the melting rate increases by 45% and 52%, respectively. Nitsas and Koronaki [15] made organic PCM better at transferring heat by adding Cu and Al_2O_3 nanoparticles to it. The study revealed that although adding hybrid Cu-Al_2O_3 nanoparticles at 0.165–0.816% boosted the melting rate by 10.8%, adding Cu nanoparticles at 0.165% enhanced it by 25.3%. Darzi et al. [16] investigated numerical PMC melting and solidification rates within the annulus by using nanoparticles and fins. Their results exposed that, more than the rate of melting, the usage of fins speeds up solidification. Besides, fins impede free convection during melting, unlike nanoparticles. According to a new study by Kadhim et al. [17] on increasing the melting time of paraffin kind RT42 in a square cell using copper fins, making the fins longer makes them better at transferring heat, which in turn makes the charging time longer.

PCMs are typically stored in containers or moulds that have a variety of geometric configurations, including cylindrical, hemicylindrical, rectangular, spherical, and shell-and-tube [18, 19]. The melting and solidification process of PCMs is influenced by the geometry of the container, as evidenced by prior research [20]. Concise reference to prior research on the thermal properties of PCMs in shell-and-tube configurations for latent heat storage applications. Investigations were implemented to ascertain the impact of material characteristics on the rates of solidification and dissolving, as well as on thermal efficiency. The solidification and melting properties for PCM in a fin and tube heat exchanger were investigated by Rahimi et al. [21] through experimental results. The PCM R35 (cube) is inserted into the heat exchanger and filled with water between the fins and the tubing. The findings indicated that the dissolving time decreased as the temperature of the water passing through the conduit increased. Tao et al. [22] created 3D simulation models for shell and tube-type latent storage systems with and without convection in order to investigate the impact of PCM layout and unrestricted convection on charging and discharging. Under identical conditions, their investigations showed that the tube side experiences a greater heat storage rate than the shell side, producing correspondingly a 25.4% and 36.6% decrease in melting time without and with free convection, respectively. Furthermore, they claim that free convection has no effect on discharge performance (solidification). To investigate the PCM solidification process in a partially filled and filled-up cylindrical tube, Bechiri and Mansouri [23] suggested a numerical study. Although the tube's top section was cleaned, a certain volume of air was allowed to let PCM expand in volume. Their results revealed that every changing factor directly affected the melt. Liang et al. [24] investigated the flow under the main annulus-side PCM-packed double concentric tube under varying flow

conditions and key parameters. These covered the form of the energy storage tube, its length-to-diameter ratio, and the volume ratio of PCM. They also mentioned there is an optimal volume fraction of PCM and that an efficient energy storage ratio is increasing with increasing the length-diameter ratio of the tube. Each of these were points they raised. Other publications focused more on speeding up PCM charging and discharging in these thermal storage devices and heat transfer. Mahdi et al. [25] introduced a new concept of PCM container suitable for Latent Heat Thermal Energy Storage (LHTES) by using double-tube helical-coiled tube. They used a 3D numerical model to study the convective phenomena during PCM melting; thus, the attainment of the suggested design was compared with the horizontal and vertical straight double-tube systems but with the same cross-sectional area. In relation to the horizontal and vertical systems, they determined that the suggested method reduces the entire melting time by 25.7% and 60%, respectively. By means of three-dimensional simulations, Wooszyn et al. [26] proposed novel double-tube LHTES units by comparing the melting time and exergy efficiency of the PCM melting process for eight variants of the system. One of the eight designs notably reduced the PCM melting time by 76%, which was better than the 66% decrease in the horizontal and 53% reduction in helically coiled tubes when it came to comparing their suggested TES units. Qaiser et al. [27] conducted thorough experimental and computational research using multi-tubes and optimized the shell to increase heat transmission in a latent heat storage system. The selected PCM, stearic acid, fills the steel shell; water, the Heat Transfer Fluid (HTF), fills the copper Y-fin tubes. Regarding their results, they revealed that, when compared to the basic arrangement of one tube placed in the center of the shell, applying the vertical double-tube configuration and the V-shaped triple-tube design reduces the entire melting time by 27%, 21.7%, and 7%, respectively. Changing the circular crust for elliptic and triangular parts also lessens the total melting time. Abderrahmane et al. [28] used numerical techniques to improve the thermal performance of a horizontal shell-and-tube heat exchanger by adding TES materials and redesigning the tubes. Whereas the tube consists of a fine-waved (trefoil-shaped) tube, the shell consists of a circular segment tube. Paraffin wax lines the shell as copper nanoparticles and PCM are added to improve heat conductivity. Their findings show that copper nanoparticles improve melting rates and thermal performance. Thermal performance is much influenced by the placement of the fin as well. Sardari et al. [29] conducted a numerical study to assess the performance of the melting process in a PCM-based heat storage system within a vertical cylindrical container incorporating copper metal foam, focussing on optimising design parameters to enhance practical application performance and minimise energy waste. The copper foam-PCM unit demonstrated a reduction in melting time exceeding 85% compared to the PCM alone. Tiji et al. [30] numerically investigate the impact of T-shaped fins on the melting of PCM within vertical triple-tube storage systems. The effects of T-shaped fins on the melting of PCM are analysed to determine the optimal scenario. The results indicate that T-shaped fins enhance the melting performance of PCMs, with the fin body being the contributing factor rather than the head. The proposed T-shaped fin did not enhance melting at the base of the PCM domain. The ideal case of the T-modified-shaped fin is compared with the No-Fin, Uniform-Fin, and Optimum T-shaped fin configurations utilising a flat fin. The melting time for the T-modified Fin case was determined to be 1882s, representing

reductions of 59.6%, 38.4%, and 33.6% compared to the no-fin, uniform-fin, and T-fin cases, respectively, in terms of performance and energy efficiency.

The shell-and-tube configuration remains one of the most widely adopted geometries for latent heat TES systems due to its compactness and high surface area-to-volume ratio [31, 32]. Prior studies have evaluated different configurations, flow conditions, and structural modifications to enhance heat transfer as mentioned earlier. However, one important factor has been largely overlooked: the insulating effect of air layers surrounding the inner tube in horizontal double concentric systems. Most existing studies assume ideal thermal contact between components, without considering trapped air layers that could influence heat transfer dynamics. Only a few recent works begin to touch on this factor, and none have quantitatively examined how varying air gap thickness affects PCM melting in this geometry. This represents a significant research gap, particularly in systems where imperfect contact or manufacturing tolerances introduce insulating layers unintentionally.

This study presents a novel numerical investigation of the impact of air layers (1 mm and 2 mm) surrounding the heated inner tube in a horizontal double concentric tube on the melting behavior of paraffin wax (RT42). Using a 2D Computational Fluid Dynamics (CFD) model in ANSYS/FLUENT 16, the study analyzes temperature distribution, velocity profiles, and melting fraction evolution to quantify the effect of air layer thickness on thermal performance. The main objective of this study is to determine how internal air gaps affect melting time, thermal resistance, and overall efficiency of PCM-based TES systems in horizontal shell-and-tube configurations. This aims is to provide practical insights for improving real-world system design where such air layers are present.

2 Methodology

2.1 Proposed model

The following is the proposed model as explained in the Fig. 1 which shows the horizontal concentric shell-and-tube with circular cross-section. The shell has a diameter of 50 mm and the tubes have a diameter of 20 mm; both are of copper. The shell side is the side which is charged with the PCM and the tube side has stagnant air at a temperature greater than the required melting temperature of the PCM. The shell is thermal insulated with the surrounding outside and it will have the following design. The first layer of air is 1 mm thick further while in a modified configuration the layer is 2 mm thick.

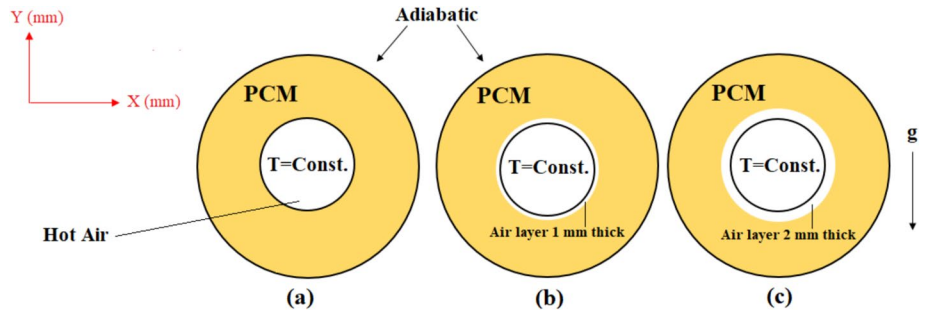


Fig. 1 Schematic of the three configurations of the horizontal double concentric tube TES system with paraffin wax (RT42) as PCM. The inner copper tube is maintained at a constant temperature. **a** No air layer, **b** 1 mm air layer, **c** 2 mm air layer

2.2 Assumptions

Before introducing the governing equations, the following assumptions were made to simplify the numerical model:

- The flow is laminar, two-dimensional, unsteady, and incompressible.
- No heat is exchanged with the surrounding environment (adiabatic outer shell).
- Thermal properties of the PCM (RT42) are constant for both solid and liquid phases.
- The air layer is separated from the PCM by a thin wall with negligible thickness.
- Viscous dissipation is negligible.
- Phase change occurs at a fixed temperature range (mushy zone formulation).

Before presenting the subsequent subsections, Fig. 2 provides a visual representation of the overall methodology used in this study. The flowchart outlines the main

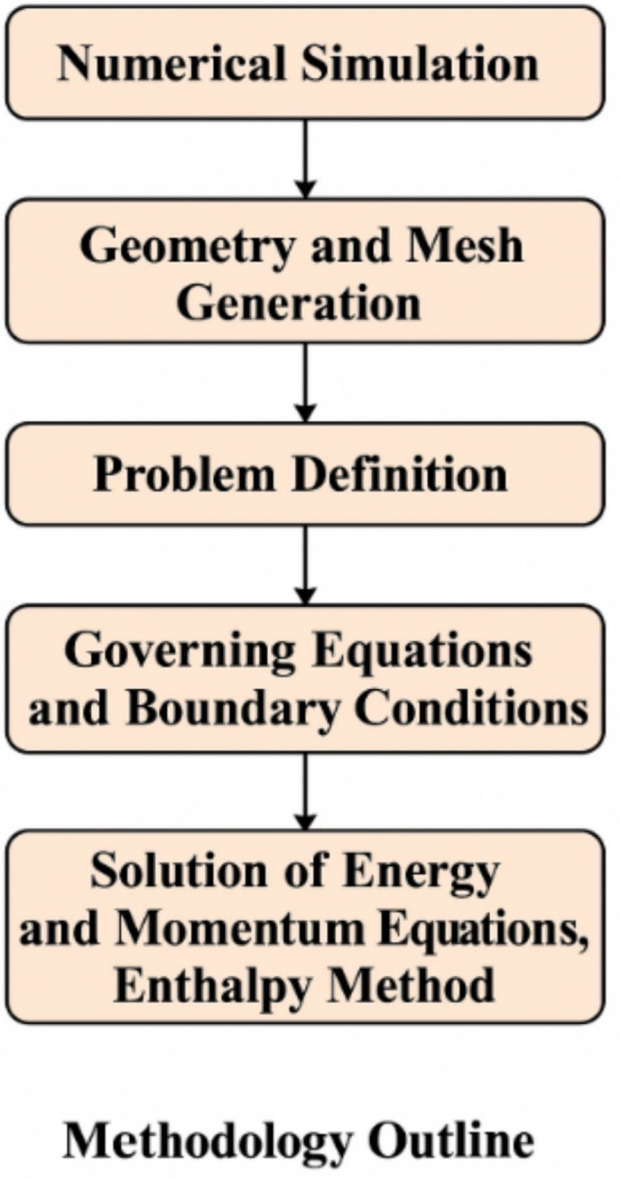


Fig. 2 Flowchart of the numerical model outlining the key steps involved in the CFD simulation of PCM melting in the horizontal double concentric tube system with or without air layers

computational steps involved in modeling the melting behavior of paraffin wax (RT42) in a horizontal double concentric tube configuration. It includes the setup of the geometric model, mesh generation, specification of material properties, application of initial and boundary conditions, and implementation of the enthalpy–porosity technique for phase change simulation. The flow then proceeds through numerical solution procedures in ANSYS FLUENT, followed by data extraction and result analysis. This structured schematic enhances clarity and offers a step-by-step view of the simulation workflow used to investigate the effect of air layers on thermal performance.

2.3 Governing equations

The numerical analysis is what makes it feasible to forecast specifics of the melting processes that take place in the shell. This capacity is made possible by the mathematical modeling. Additionally, it was determined that the flow was two-dimensional, laminar, unstable, and incompressible during the experiment. The modeling of melting processes makes the assumption that both the liquid and the solid phase are homogenous, isotropic, and in thermodynamic equilibrium at the phase boundary. This is a postulation that is made in the modeling of the melting processes. It was decided that the area under the curve for the PCM would be located on the line that connects enthalpy and porosity. Some of the melting processes of PCMs are thought to be a group sin because they are nonlinear, temporal conduct and the interface between the solid and liquid is always shifting. Equations (1), (2), and (3) are employed in the simulation of PCMs' melting process. These equations represent continuity, momentum, and energy, which are all present in partial differential equations [33–35]:

Continuity equation is ensures mass conservation and can be expressed by Eq. (1):

$$\frac{\partial \rho}{\partial t} + \nabla . (\rho V) = 0 \tag{1}$$

Momentum equation (fluid motion + buoyancy) governs the fluid flow induced by buoyancy during phase change:

$$\frac{\partial (\rho V)}{\partial t} + \nabla . (\rho V) = -\nabla P + \mu \nabla^2 V + \rho g + S \tag{2}$$

Energy equation (heat transfer + phase change) captures both sensible and latent heat transfer during melting:

$$\frac{\partial}{\partial t} (\rho E) + \nabla . (\rho V H) = \nabla . (K \nabla T) \tag{3}$$

Total enthalpy:

Sum of sensible enthalpy (h) and latent heat (ΔH) is the specific enthalpy H:

$$H = \ h + \Delta H \tag{4}$$

where, Sensible enthalpy:

$$h = h_{ref} + \int_{T_{ref}}^{T} C_p dT \tag{5}$$

Latent enthalpy:

$$\Delta H = \beta L_f \tag{6}$$

Here, β is the liquid melting fraction, and L_f is the latent heat of melting for the liquid phase. Latent heat of fusion is zero to one for solids and liquids, respectively. The following is the equation for the liquid melting fraction:

$$\beta = \begin{cases} 0 \text{ solidus} & \text{if } T < T_s \\ 1 \text{ liquidus} & \text{if } T > T_l \\ \frac{T-T_s}{T_l-T_s} & \text{if } T_s \leq T \leq T_l \end{cases} \tag{7}$$

Source term in momentum equation:

The source term S in the momentum equation is utilized to represent the damping force of Darcy's law. This effect is introduced in the equation to assess the effect of phase shift and convection on the system. Such a quantity is referred to as the source term in the momentum equation:

$$S = \frac{C(1-\beta)^2}{\beta^3} V \tag{8}$$

The morphology of the melting region follows from the coefficient. Here V stands for velocity and C for a semi-solid constant zone. This particular fixed is a large number, usually approximately (10^4–10^7) [36]. In the present study, C is taken to be constant and is given as (10^5).

Each of these equations is solved numerically using the finite volume method. Melting is tracked based on the value of β, with flow limited in solid regions by the source term S. The simulations were run for each case (no air layer, 1 mm air, 2 mm air) to assess the impact of thermal resistance on melting behavior.

In the configurations involving air layers (1 mm and 2 mm), the air is modeled as a separate, stationary region between the inner copper tube and the PCM domain. Since air does not undergo phase change and is assumed to be stagnant, only transient heat conduction is considered in this region. Therefore, the governing equation used for the air layer is:

$$\frac{\partial T}{\partial t} = \frac{k_{air}}{\rho_{air} Cp_{air}} \nabla^2 T \tag{9}$$

No velocity terms are included in this zone due to the stagnant nature of the air. At the interfaces between the tube–air and air–PCM, conjugate boundary conditions are applied to maintain physical accuracy:

Continuity of temperature:

$$T_{tube} = T_{air} \text{ and } T_{air} = T_{PCM}$$

Continuity of heat flux:

$$-k_{tube}\left(\frac{\partial T}{\partial n}\right)_{tube} = -k_{air}\left(\frac{\partial T}{\partial n}\right)_{air} = -k_{PCM}\left(\frac{\partial T}{\partial n}\right)_{PCM} \tag{10}$$

Table 1 Thermophysical characteristics of paraffin wax RT42. [37, 38]

Properties	RT42
Density (kg/m^3)	760
Specific heat capacity (J/kg K)	2000
Thermal conductivity (W/m K)	0.2
Dynamic viscosity (kg/m s)	0.02351
Thermal expansion rate (1/K)	0.0005
Latent heat (J/kg)	165,000
Melting temperature (K)	311.15–315.15

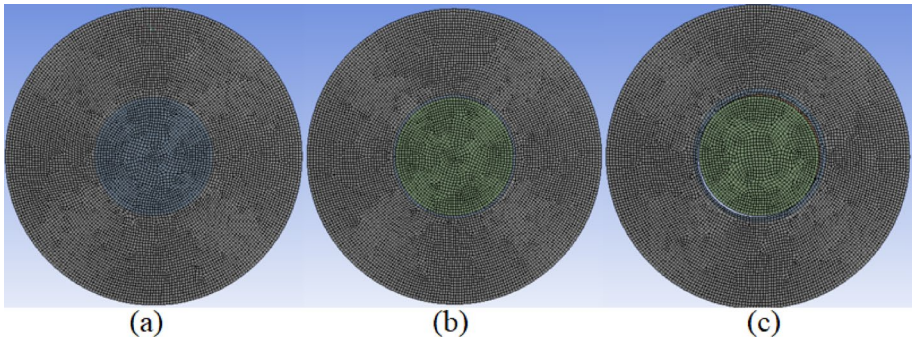


Fig. 3 Finite element mesh distribution used for the numerical simulation: **a** no air layer, **b** 1 mm air layer, **c** 2 mm air layer

2.4 Boundary conditions

Inside the shell of the horizontal double concentric tube system, the PCM, paraffin wax RT42, is heated by conduction and convection from the inner surface of a centrally placed copper tube. In the simulation, the inner tube wall is maintained at a constant temperature of 353 K, providing a steady heat source to initiate melting. A no-slip velocity condition (V = 0) is applied at this surface, ensuring the PCM adheres to the boundary with no relative motion. Similarly, the outer shell wall is modeled as adiabatic, preventing any heat loss to the surroundings, and is also treated with a no-slip condition. The PCM is initially solid, uniformly at 313 K, and at rest throughout the domain (V = 0). As heating begins, melting initiates at the tube interface and progresses outward, driven initially by conduction and later enhanced by natural convection in the liquid PCM due to buoyancy forces. These flow patterns evolve dynamically based on local temperature gradients and are resolved using the enthalpy–porosity method. Proper specification of velocity boundary conditions is critical to accurately represent the transition from conduction-dominated to convection-influenced melting. The thermophysical properties of RT42 used in the simulation, including latent heat and thermal conductivity, are summarized in Table 1. The mesh distribution used for spatial discretization of the domain is shown in Fig. 3.

2.5 Mesh test and model validation

Mesh independence evaluation in CFD simulations is one of the most critical steps to ensuring thermal system reliability and effectiveness. In practice, researchers take a number of steps in concave areas, clean up the computational mesh, conduct convergence tests, and use some quantitative metrics to ensure the stability of results as the mesh density increases. Such an empirical approach is crucial to actual applications like

electronic chip thermal management, HVAC designs, and automotive cooling systems that require an accurate model of heat transfer dynamics for optimal outcomes. Study of mesh independence has been a major first step in CFD research, mainly aimed at examining the effect of changing mesh densities on phase change behavior in particular geometric configuration. Four distinct grid densities (34,567, 36,789, 38,765, and 40,987) corresponding to the quantity of elements are analyzed. These densities were meticulously chosen to suit many computational options. Consequently, the computed results did not show significant effects from the choice of network density, indicating the network's independence. Because of the quick processing time at Fig. 4, the lowest element number (34,567) was carefully chosen for the ensuing simulations.

It is important to note that the mesh configuration used in the simulations was consistent across all three cases—no air layer, 1 mm air layer, and 2 mm air layer—with only minor adjustments to account for geometric differences in the presence of the air gap. The mesh density was refined near the inner tube surface and PCM interface in all configurations to accurately capture temperature gradients and melting fronts. Although the total number of elements varied slightly due to domain size (e.g., 34,567 elements for the base case and up to 40,987 for the 2 mm air layer), the element sizing and boundary layer refinement were kept constant to ensure comparability between the cases. Therefore, there is no significant difference in mesh structure or quality between the three types presented in Fig. 3, and any variations are purely a function of domain geometry rather than mesh strategy.

To further improve the numerical simulation framework's dependability, a comprehensive validation procedure was applied. The simulation method now includes an additional feature that enables simulation of the complexity of fluid components and geometry. Esapour et al. [39] conducted a ground-breaking study that investigated the intricacies of fluid and thermal movement during the phase transformation of PCM in a vertical cylindrical tube, prompting numerous modifications to the computational framework. The results from the optimized simulation code and those obtained by humans are compared thoroughly and reviewed in order to show that there was a

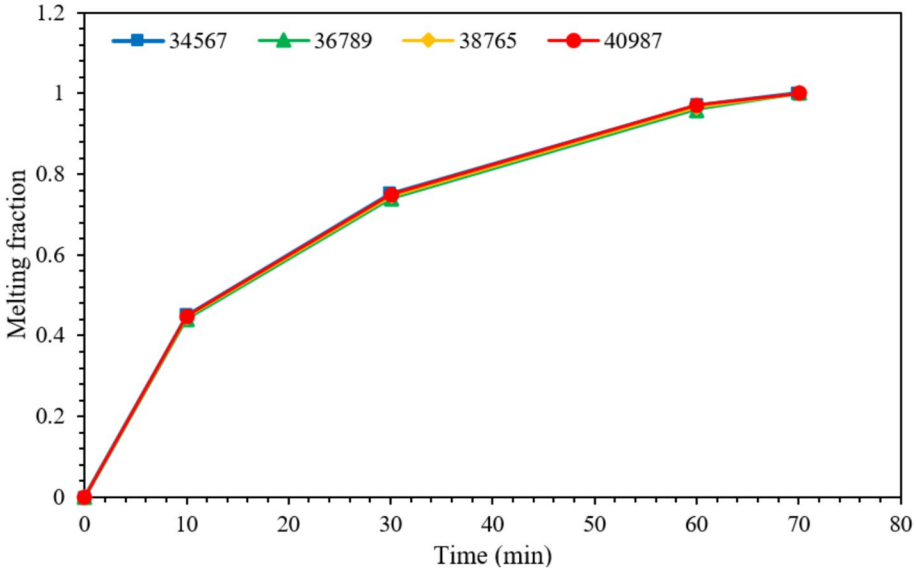


Fig. 4 Grid independency test

surprising amount of agreement between the two data sets. The comparison showed the accuracy and flexibility of the revised simulation code, that only a tiny change had to get made, even with the stringently different computational methods and model parameters shown in Fig. 5.

Specifically, the predicted complete melting time in the reference study was 4800 s, whereas this simulation yielded 4440 s for the same boundary and material conditions. Using these values, the following error metrics were calculated. Root Mean Square Error (RMSE) in the melting time was about 360 s, while the percentage deviation in melting time was about 8.1%. These metrics indicate that the simulation deviates by only 8.1% from the reference case, demonstrating strong quantitative agreement and verifying the accuracy of the modeling approach. This level of deviation is considered acceptable for CFD-based melting models involving natural convection and latent heat storage. It is worth noting that the percentage deviation between the four grid densities does not exceed 1%.

3 Results and discussion

The melting of paraffin wax (RT42) in the horizontal double concentric tube system is governed by a combination of heat conduction, natural convection, and buoyancy-driven flow. Initially, heat is transferred from the heated inner tube to the solid PCM primarily through conduction, forming a melt layer adjacent to the tube surface. As melting progresses, thermal gradients generate density differences in the liquid PCM, initiating convective motion that enhances heat transfer. The air layer, when present, acts as a thermal barrier that reduces the effective heat flux from the inner wall, delaying both melting initiation and the onset of convection. With increasing air layer thickness, the melting process becomes more conduction-dominated due to weakened buoyancy effects. Consequently, the overall melting performance depends on the interplay between thermal conductivity, natural convection strength, and geometric insulation effects, all of which affect temperature distribution, melt front dynamics, and latent heat absorption efficiency.

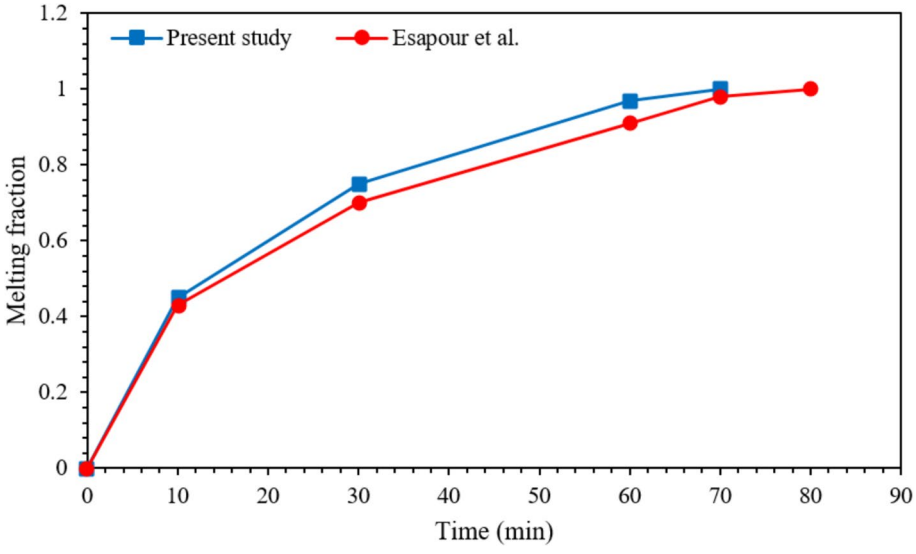


Fig. 5 Comparison of the current investigation with Esapour et al. study [39] concerning the entire melting time

To simulate the melting behavior described above, this study adopts the enthalpy–porosity method, a robust numerical approach for modeling phase change with natural convection. This method enables the simultaneous resolution of heat transfer, fluid flow, and phase interface dynamics without explicit interface tracking. A momentum damping term is incorporated into the Navier–Stokes equations to suppress velocity in solid and mushy regions, ensuring a smooth transition from solid to liquid behavior. The energy equation accounts for latent heat through an enthalpy formulation that updates local phase fractions based on temperature. This framework is implemented using ANSYS Fluent, with boundary and initial conditions defined to match physical constraints. The modeling assumptions, including incompressible flow, constant thermophysical properties, and negligible radiation, are outlined in Sect. 2.4 and are consistent with established literature [39–41]. The accuracy of this model is validated both qualitatively and quantitatively against reference data, confirming its suitability for capturing the thermal behavior of PCM melting in geometries with and without air layers.

In order that achieve optimal performance of heat recovery processes and renewable energy systems, there is a need for a full comprehension of the behavior of PCMs in TES system. This knowledge is crucial to take the best advantage of these systems. The phase change process, which directly influences how (PCMs) absorb, store, and release thermal energy, is significantly influenced by environmental elements such as the ambient temperature, humidity, and sun radiation. These environment factors play a vital part in the process. Changes in temperature can alter the phase transition timing, while factors like humidity and solar radiation can influence the system's insulation and lead to energy loss. Thus, accounting for these conditions during the design phase is essential to ensure the TES system performs efficiently in various environments.

TES systems, which are employed in applications such as smart buildings, solar power setups, and power plants, require a detailed examination of the effects of external factors on geometry and boundary conditions. This study specifically looks at three scenarios:

1. Paraffin wax is melted inside a shell without an air layer, in the first case.
2. A 1 mm air layer is introduced around the wax, in the second case.
3. A 2 mm air layer is considered, in the third case.

To compare these cases effectively, the temperature distribution of the paraffin wax within the shell was analyzed at dissimilar time intervals throughout the melting process. Also, the velocity distribution and the melting fraction were investigated, thus offering a complete insight on how those factors affect the system efficiency and performance under different environmental and design conditions.

For each case, Figs. 6, 7, and 8 show how the paraffin wax inside the shell changed temperature. In example one, it is found that heat conduction from the hot surface causes the paraffin wax temperatures in the vicinity of the hot tube surface to rise significantly, and that the temperatures fall as one proceeds away from the hot surface. Also noted in the temperature profiles in the vicinity of the warm surface in the cases two and three are that temperatures fall with the thick of the air layer growing. The thermal resistance of the air layer impedes the heat flux to the paraffin wax, and the resistance grows when the thickness increases [42, 43]. As time goes on, the temperature in the paraffin wax layers farthest from the hot surface increases due to free convection and continuous thermal conductivity. The strength of the free-convection flow is larger in the upper-level areas

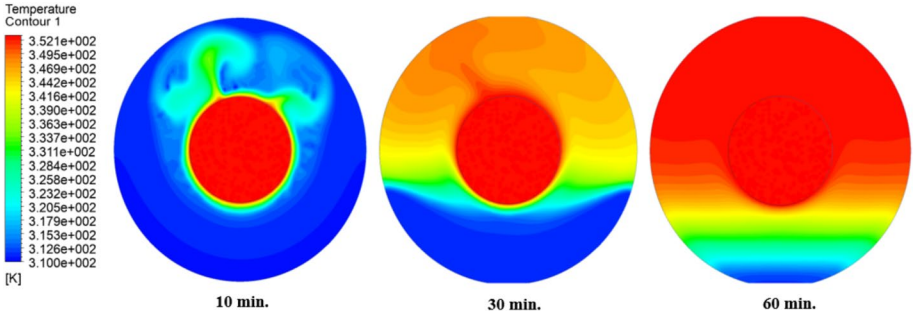


Fig. 6 Paraffin wax temperature contours inside the shell at three different times throughout the air layer-free melting process

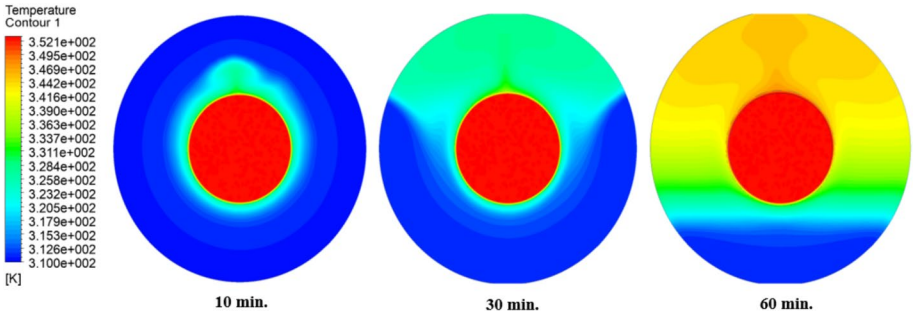


Fig. 7 Paraffin wax temperature contours within the shell at three distinct intervals throughout the melting process, accompanied by a 1 mm air layer

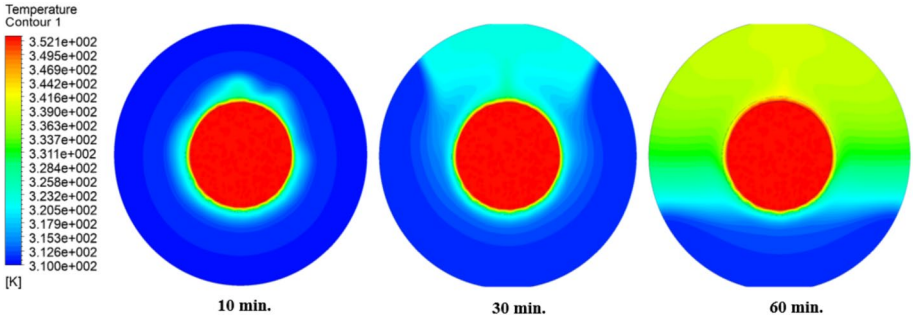


Fig. 8 Paraffin wax temperature contours within the shell at three different times throughout the melting process with a 2 mm air layer

above the tube, especially in case one, therefore it leads to a rise in the temperature of the upper part of the shell, especially near the hottest surface. When looking at the paraffin wax temperatures in all three situations, a significant disparity becomes apparent. It was noted that the temperature in over 75% of the shell area of case one attained or exceeded the temperature required for the melting of paraffin wax (315 K) after 60 min. In case two, the temperature level of the paraffin wax decreases compared to the previous case, at 60 min have passed since the melting process, it has not reached the previous temperature level. The paraffin wax temperature level decreases further in the case three.

The concentric temperature patterns in Figs. 6, 7 and 8—where the highest temperatures localize near the inner tube—result from conduction-dominated heat transfer in

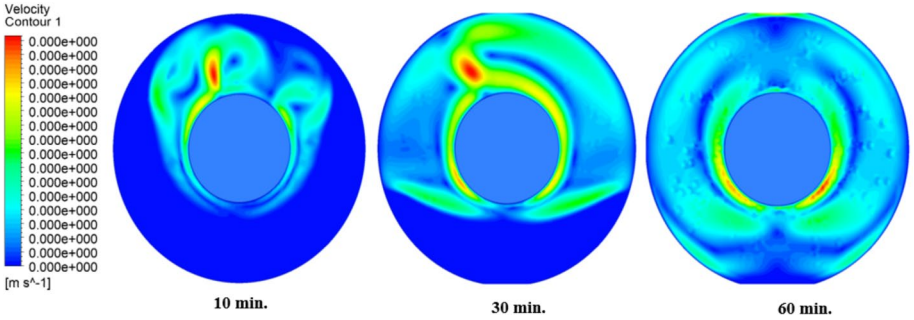


Fig. 9 Paraffin wax velocity contours within the shell at three different times throughout the melting process without an air layer

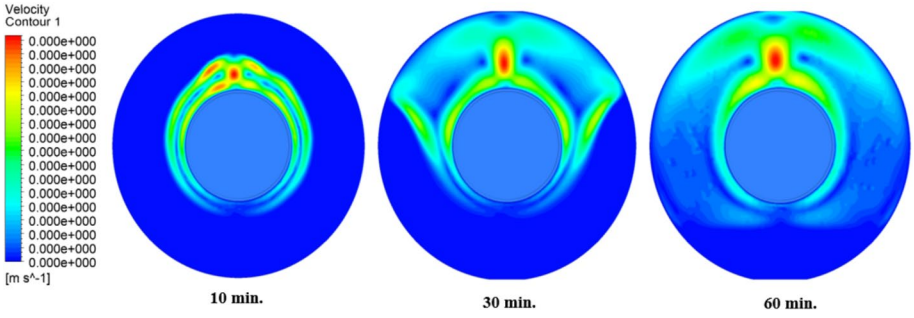


Fig. 10 Paraffin wax velocity contours within the shell during melting with a 1 mm air layer during three time intervals

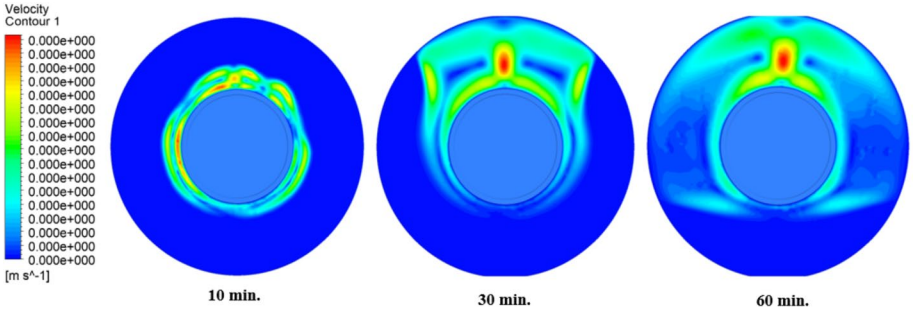


Fig. 11 Paraffin wax velocity contours inside the shell during melting with a 2 mm air layer at three different times

early stages, creating steep thermal gradients. While natural convection later redistributes heat upward (evident in the upper-region temperature rise), the air layer's thermal resistance preserves this disparity by delaying convective mixing. This explains why the hottest zones remain constrained near the tube wall, while outer regions lag in temperature rise, particularly in Cases 2 and 3 where thicker air gaps amplify insulation effects.

Figures 9, 10, and 11 illustrate the variety of velocities observed within the shell for each of the three different scenarios. As the solid paraffin wax begins to melt, the resulting liquid layers slide and rise due to buoyancy forces, initiating natural convection. In Case 1, velocity profiles appear near the heated tube surface as early as 10 min, particularly on the top side, indicating the onset of melting and fluid motion. After around 20 min, velocity becomes more pronounced near the heated wall, suggesting intensified

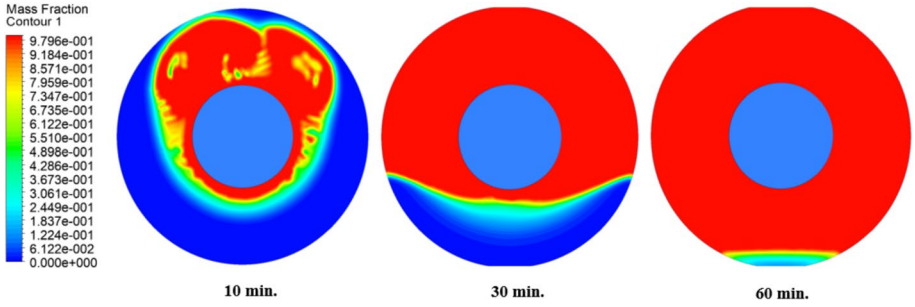


Fig. 12 Phases of the paraffin wax melting process within the shell over the course of three-time intervals without an air layer

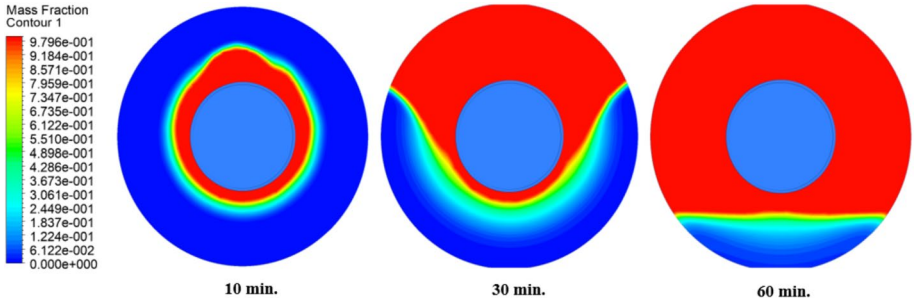


Fig. 13 Phases of the paraffin wax melting process across three-time intervals within the shell with a 1 mm air layer

heat absorption. By 30 min, strong velocity contours are evident across the entire shell, signaling that most of the PCM has transitioned to liquid.

At 10 and 30 min, the velocity contours are symmetrically distributed toward the upper region of the shell, indicating well-developed natural convection loops formed by strong thermal gradients. However, at 60 min, the velocity field becomes visibly asymmetric and less organized. This is due to a significant reduction in thermal gradients, as much of the PCM—especially in the upper regions—has already melted. The remaining solid PCM tends to accumulate in the lower part of the shell, disrupting fluid flow symmetry and increasing resistance to buoyancy-induced circulation. This weakened convection and irregular melt–solid interface lead to the observed misalignment, which is a typical behavior in late-stage melting systems governed by diminishing thermal forces.

In Cases 2 and 3, the appearance of velocity contours is delayed compared to Case 1, with the delay more pronounced in Case 3 due to the presence of the air layer. The air gap acts as an insulating barrier, reducing heat transfer between the heat transfer fluid (HTF) and the PCM. This insulation helps regulate the phase change rate, prevents overheating, and supports more uniform melting. Additionally, the air layer reduces heat loss to the environment, improving overall thermal efficiency and energy retention during extended storage periods.

Figures 12, 13 and 14 illustrate the steps of the melting fraction formation with the time staying in the shell. The paraffin wax melting process starts from the region adjacent to the hot tube surface because of thermal conductivity. After 10 min, it is noticed that the melting fraction in case one is more than the melting fraction in case two, and hence greater than the melting fraction in instance three, which has the least melting fraction. After 30 min, the melting percentage rises, and the solid–liquid barrier shrinks.

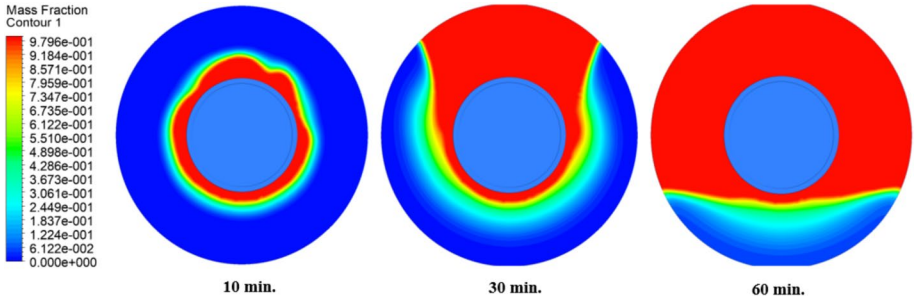


Fig. 14 Phases of the paraffin wax melting process across three-time intervals within the shell with a 2 mm air layer

In addition to the conduction effects, free convection has an effect here. During this time period, the melting percentage is always in the upper half of the shell due to buoyancy force lift liquid layers upwards. In comparison, during this period of time, almost two-thirds of the solid paraffin wax inside the shell melted in instance one, half of it melted in case two, and one-third melted in case three. After 60 min, the paraffin wax within the shell had nearly totally melted in the first example. In the other circumstances, a portion of the paraffin wax remains solid at the bottom, although the solid–liquid contact thins, especially in example two.

Each parameter studied influences the melting dynamics through a specific physical mechanism. The presence of an air layer introduces additional thermal resistance between the heated tube wall and the PCM, reducing the initial heat transfer rate and delaying the melting process. However, once the PCM near the interface begins to melt, the effect of natural convection—driven by buoyancy forces—enhances heat transfer in the upper regions. The thickness of the air layer modifies this interaction by delaying the onset of convection and shifting the melting dominance toward conduction. Additionally, the melt fraction progression over time reflects the balance between these two heat transfer modes, as well as the insulation impact imposed by the air gap. These parametric effects collectively determine the thermal response and energy absorption efficiency of the PCM.

Figure 15 provides a definitive comparison between the three examples that were investigated, which are signified by the phases of attaining to complete paraffin wax melting time in the shell. This analysis is presented to facilitate a clear visualisation and comparison of the data. It is evident that the duration required in the first instance is less than that of the second case, and subsequently, the third case, a pattern that holds true for all fractions as well. This becomes apparent not solely when the melting fraction attains a value of 1. In the first scenario, the duration required to complete the melting process was approximately 70 min. In the second scenario, this duration extended to around 90 min, while in the third scenario, it reached about 110 min. The total duration for melting was observed to rise by 28.57% with the introduction of a 1 mm thick air layer, and by 57.14% with the addition of a 2 mm thick air layer. One could assert that augmenting the thickness of the air layer surrounding the hot tube surface by 1 mm will prolong the duration required for complete paraffin wax melting within the shell. It is important to recognise that altering the heat transfer medium (air) or introducing a flow velocity within the tube is anticipated to yield entirely distinct outcomes [44, 45]. This may be regarded as prospective research that complements the current study.

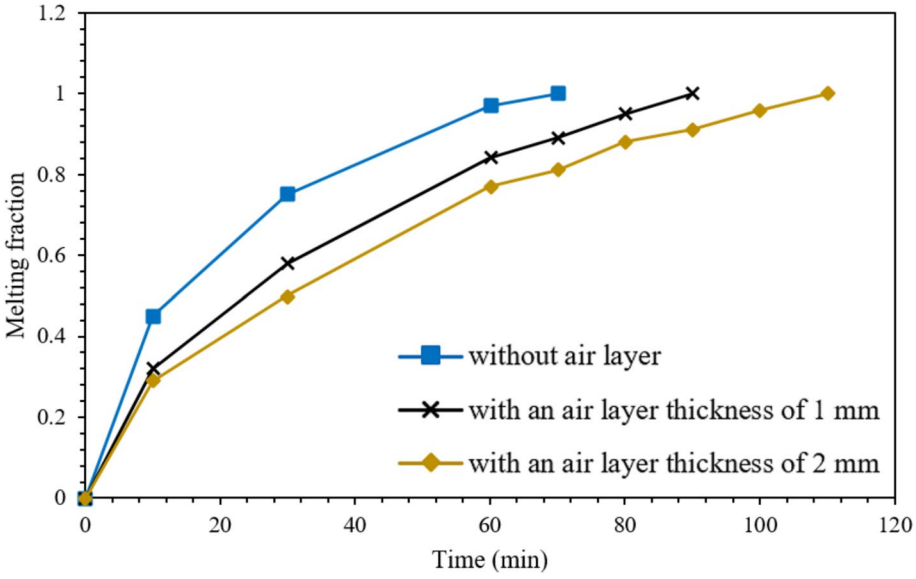


Fig. 15 Melting process for the three cases

Although the air layer slows the initial melting by acting as an insulating barrier, it also reduces radial heat loss and sustains a more stable temperature gradient across the PCM domain. This delayed yet extended heating leads to more complete melting over time, particularly in the upper and central regions of the shell. As shown in Fig. 15, the cases with 1 mm and 2 mm air layers exhibit higher melt fractions in the later stages of the simulation compared to the base case, due to the accumulated thermal energy and slower heat dissipation. The presence of the air layer helps maintain the PCM within the effective melting temperature range for longer periods, thus increasing the total amount of phase change achieved.

4 Conclusions

This study numerically investigated the melting behavior of paraffin wax (RT42) in a horizontal double concentric tube system using the enthalpy–porosity method, with a particular focus on the effect of air layer thickness. The key findings are summarized below:

- The introduction of an air layer between the heated inner tube and the PCM introduces thermal resistance, which slows down the melting process by reducing heat flux from the hot wall.
- The total melting time increased by approximately 28.57% for the 1 mm air layer and 57.14% for the 2 mm air layer compared to the no-air-layer case, indicating the insulating effect of the air gap.
- Temperature distributions revealed that the air layer causes the PCM to remain in the melting range for a longer duration, leading to a more gradual and extended melting process. This results in better heat retention but at the cost of reduced thermal response speed.
- The presence of the air layer also suppresses natural convection currents within the molten PCM, particularly in the upper regions, shifting the heat transfer mode toward conduction-dominated behavior as the air gap increases.

- These findings highlight that while adding an air layer reduces the rate of melting, it may be beneficial in applications where thermal regulation, delayed heat release, or thermal insulation are desired.

Future research may focus on optimizing the thickness of the air gap or investigating PCM performance under cyclic heating conditions to improve system efficiency and practical applicability.

5 Limitations and future work

5.1 Limitations

- The above study was made with the help of two-dimensional numerical model and particular boundary conditions. While this is informative it does not necessarily give a true representation of three-dimensional heat transfer and phase change in practical applications.
- In the simulations, the thermal and physical properties of paraffin wax namely, RT 42 was assumed to be invariant. Though, in real-life applications, these properties can be temperature and phase dependent which may lead to error in results.
- The study failed to take into consideration the impact of thermal contact resistance of the PCM with the air layer. This resistance could affect the overall heat transfer and melting pattern and this was something that could probably require further studies in the future.
- It is pertinent to mention here that while analyzing the impact of air layers only the effect which they have on the melting of ice was taken into account. Other parameters within an environment including fluctuating ambient temperatures and external convection currents were out of the research study's range.
- The study assumes ideal adiabatic conditions, but real-world environments like fluctuating ambient temperatures, humidity, or external convection may alter PCM performance. For instance, heat loss to colder surroundings could slow melting, while high ambient temperatures might accelerate it.

5.2 Future work

- Three-dimensional models would provide more precise information regarding the melting and heat transport processes of PCM in various geometries.
- In future research, temperature-dependent material properties should be used to see how thermal contact resistance between layers and parts of the thermal storage system affects how well they work.
- If the thermal performance of PCMs was studied in situations with changing humidity levels, temperatures, and convection currents from the outside, it might give a more accurate picture of how they work in different settings.
- Experimental study to back up numerical findings was recommended for model improvement and improved outcomes. Experimental data and simulation results can be compared to detect simulation errors and inaccuracies.
- The combination of fins, nanoparticles, optimised shapes, and air layers can provide a synergistic effect that enhances heat transport and storage.
- Evaluate environmental impacts on PCM efficiency under dynamic conditions.

Thus, if these limitations are eliminated, and the outlined future work is performed, the knowledge and use of PCMs in TES systems for RES may be enhanced, and more effective and feasible solutions can be achieved.

List of symbols

h	Sensible enthalpy J/kg
H	Total enthalpy (sensible + latent) J/kg
ΔH	Latent heat of fusion J/kg
β	Liquid fraction (0 for solid, 1 for liquid)
L_f	Latent heat of fusion of PCM J/kg
T	Temperature K
V	Velocity vector m/s
C	Mushy zone constant
S	Source term in momentum equation (Darcy force) kg/(m^2 s^2)
t	Time s
ρ	Density kg/m^3
μ	Dynamic viscosity Pa s
k	Thermal conductivity W/m K
cp	Specific heat capacity at constant pressure J/kg K
g	Gravitational acceleration m/s^2

Abbreviations

PCM	Phase Change Material
TES	Thermal Energy Storage
CFD	Computational Fluid Dynamics
LHTES	Latent Heat Thermal Energy Storage
HTF	Heat Transfer Fluid
ANSYS	Analysis System (commercial CFD software)
2D	Two-Dimensional
RMSE	Root Mean Square Error
RT42	Commercial paraffin-based PCM (melting ~ 42 °C)

Acknowledgements
The authors wish to express their sincere gratitude to Al-Mustaqbal University, Hillah, Iraq, for their support during the preparation of this research. Additionally, the authors are deeply indebted to University of Miskolc, Hungary, for their assistance, support this research.

Author contributions
K.A. H: Methodology, Formal analysis, Investigation, Resources, Writing—Original Draft, Writing—Review & Editing. R.H. R: Conceptualization, Methodology, Writing—Review & Editing. I.O: Investigation, Software, Writing—Review & Editing. S.A. K: Methodology, Writing—Original Draft, Writing—Review & Editing. A.B: Validation, Writing—Review & Editing. R.S: Validation, Writing—Review & Editing. M.A. F: Validation, Writing—Review & Editing. M.A. F: Formal analysis, Writing—Review & Editing. A.F. K: Software. F.L. R: Supervision.

Funding
Open access funding provided by University of Miskolc.

Data availability
The data that support the findings of this study are available on request from the corresponding author.

Declarations

Ethics approval and consent to participate
Not applicable.

Consent to publish
Not applicable.

Competing interests
The authors declare no competing interests.

Author details
[1]College of Engineering, University of Al Maarif, Ramadi, Al Anbar, Iraq
[2]Department of Renewable Energy Techniques, Karbala Technical Institute, Al-Furat Al-Awsat Technical University (ATU), Karbala, Iraq
[3]Department of Air Conditioning and Refrigeration, Faculty of Engineering, University of Warith Al-Anbiyaa, Karbala 56001, Iraq
[4]Institute of Physics and Electrical Engineering, University of Miskolc, Miskolc, Hungary
[5]College of Mechanical Engineering, University of Technology- Iraq, Baghdad, Iraq
[6]Laboratory of Mechanical Modelling, Energy & Materials (LM2EM), LR24ES23, National Engineering School of Gabes (ENIG), University of Gabes, Gabes, Tunisia
[7]Department of Mechanical EngCineering, King Fahd University of Petroleum and Minerals, 31621 Dhahran, Saudi Arabia

[8]IRC Sustainable Energy Systems (IRC-SES), King Fahd University of Petroleum and Minerals, 31261 Dhahran, Saudi Arabia
[9]Prosthetics and Orthotics Engineering Department, College of Engineering and Technologies, Al-Mustaqbal University, Hillah 51001, Iraq
[10]Faculty of Engineering, Kerbala University, Karbala 56001, Iraq
[11]Petroleum Engineering Department, College of Engineering, University of Kerbala, Karbala 56001, Iraq

Received: 7 May 2025 / Accepted: 4 November 2025
Published online: 01 February 2026

References

1. Regin AF, Solanki SC, Saini JS. Heat transfer characteristics of thermal energy storage system using PCM capsules: a review. Renew Sustain Energy Rev. 2008;12(9):2438–58. https://doi.org/10.1016/j.rser.2007.06.009.
2. Abdulghafor IA, Ali SA, Kadhim SA, Al-Mrayatee HM, Hammoodi KA. Exergy analysis of a solar heating system in indoor spaces. Int J Heat Technol. 2024;42(5):1151–558. https://doi.org/10.18280/ijht.420508.
3. Al-Yasiri Q, Alshara AK, Al Sudani M, Al Khafaji A, Al-Bahadli M. Advanced building envelope by integrating phase change material into a double-pane window at various orientations. Energy Build. 2025;328:115140. https://doi.org/10.1016/j.enbuild.2024.115140.
4. Sadiq IE, Aljabair S, Karamallah AA. Improving the charging rate and energy recovery of triplex tube heat storage-based pcm with mono/hybrid nanoparticles. Eng Technol J. 2024;42(01):206–31. https://doi.org/10.30684/etj.2023.144438.1631.
5. Al-Yasiri Q, Szabó M. Thermal analysis of concrete bricks-embedded phase change material: a case study under hot weather conditions. Case Stud Constr Mater. 2023;18:e02193. https://doi.org/10.1016/j.cscm.2023.e02193.
6. Mekki N, Ghriss O, Bouabidi A, Hammoodi KA, Kadhim SA. 4 E analysis of pyramid solar still with heat storage using different PCM layer thickness: energy, exergy, economic, and enviro-economic. J Energy Storage. 2025;130:117374. https://doi.org/10.1016/j.est.2025.117374.
7. Wu S, Yan T, Kuai Z, Pan W. Thermal conductivity enhancement on phase change materials for thermal energy storage: a review. Energy Storage Mater. 2020;25:251–95. https://doi.org/10.1016/j.ensm.2019.10.010.
8. Tyagi VV, Chopra K, Sharma RK, Pandey AK, Tyagi SK, Ahmad MS, et al. A comprehensive review on phase change materials for heat storage applications: development, characterization, thermal and chemical stability. Solar Energy Mater Solar Cells. 2022;234:111392. https://doi.org/10.1016/j.solmat.2021.111392.
9. Hammoodi KA, Abdulghafor IA, Kadhim SA, Elsheikh A, Nayyaf DR, mohsin Alsayah A, et al. Effect of air layer on PCMs melting process inside a spherical container: a numerical investigation. Results Eng. 2024;24:103088. https://doi.org/10.1016/j.rineng.2024.103088.
10. Raj JV, Harish R. Enhanced helical fin designs with sugar alcohol-based hybrid NEPCM for improved melting and thermal safety in Lithium-Ion battery. Energy Conv Manag: X. 2025. https://doi.org/10.1016/j.ecmx.2025.101032.
11. Gurgenc E, Gur M, Cosanay H, Gurgenc T, Oztop HF. Effects of position of semi-circular body on melting of a novel B4C/RT44HC PCM nanocomposite in a closed space. Case Stud Therm Eng. 2025;65:105628. https://doi.org/10.1016/j.csite.2024.105628.
12. Kadhim SA, et al. Enhancing phase change material melting in rectangular enclosures: A numerical study on the impact of fin length on heat transfer efficiency. J Braz Soc Mech Sci Eng. 2025. https://doi.org/10.1007/s40430-025-05855-9.
13. Nandi A, Biswas N. Enhanced melting dynamics of phase change material (PCM) based energy storage system combining modified fin and nanoparticles under solar irradiation. Int J Numer Methods Heat Fluid Flow. 2025. https://doi.org/10.1108/HFF-08-2024-0643.
14. Basem A, Hammoodi KA, Al-Tajer AM, Mohsen AM, Omar I. A numerical investigation of the increase in heat transfer in a half-cylindrical container filled with phase change copper rods. Case Stud Therm Eng. 2022;40:102512. https://doi.org/10.1016/j.csite.2022.102512.
15. Nitsas M, Koronaki IP. Performance analysis of nanoparticles-enhanced PCM: an experimental approach. Therm Sci Eng Progress. 2021;25:100963. https://doi.org/10.1016/j.tsep.2021.100963.
16. Darzi AAR, Jourabian M, Farhadi M. Melting and solidification of PCM enhanced by radial conductive fins and nanoparticles in cylindrical annulus. Energy Convers Manage. 2016;118:253–63. https://doi.org/10.1016/j.enconman.2016.04.016.
17. Kadhim SA, Hammoodi KA, Alshukri MJ, Omle I, Hussein KKA, Khalaf AF, et al. Enhancing the melting rate of RT42 paraffin wax in a square cell with varied copper fin lengths and orientations: a numerical simulation. Int J Thermofluids. 2024. https://doi.org/10.1016/j.ijft.2024.100877.
18. Dhaidan NS, Khalaf AF, Khodadadi JM. Numerical and experimental investigation of melting of paraffin in a hemicylindrical capsule. J Therm Sci Eng Appl. 2021;13(5):051008. https://doi.org/10.1115/1.4049873.
19. Khalaf AF, Rashid FL, Basem A, Abbas MH. Numerical study of the effect of air bubble location on the PCM melting process in a rectangular cavity. Math Model Eng Probl. 2023. https://doi.org/10.18280/mmep.100109.
20. Zayed ME, Zhao J, Li W, Elsheikh AH, Elbanna AM, Jing L, et al. Recent progress in phase change materials storage containers: geometries, design considerations and heat transfer improvement methods. J Energy Storage. 2020;30:101341. https://doi.org/10.1016/j.est.2020.101341.
21. Rahimi M, Ranjbar AA, Ganji DD, Sedighi K, Hosseini MJ, Bahrampoury R. Analysis of geometrical and operational parameters of PCM in a fin and tube heat exchanger. Int Commun Heat Mass Transf. 2014;53:109–15. https://doi.org/10.1016/j.icheatmasstransfer.2014.02.025.
22. Tao YB, Liu YK, He YL. Effects of PCM arrangement and natural convection on charging and discharging performance of shell-and-tube LHS unit. Int J Heat Mass Transf. 2017;115:99–107. https://doi.org/10.1016/j.ijheatmasstransfer.2017.07.098.
23. Bechiri M, Mansouri K. Study of heat and fluid flow during melting of PCM inside vertical cylindrical tube. Int J Therm Sci. 2019;135:235–46. https://doi.org/10.1016/j.ijthermalsci.2018.09.017.
24. Liang H, Niu J, Gan Y. Performance optimization for shell-and-tube PCM thermal energy storage. J Energy Storage. 2020;30:101421. https://doi.org/10.1016/j.est.2020.101421.

25. Mahdi MS, Mahood HB, Mahdi JM, Khadom AA, Campbell AN. Improved PCM melting in a thermal energy storage system of double-pipe helical-coil tube. Energy Convers Manage. 2020;203:112238. https://doi.org/10.1016/j.enconman.2019.112238.
26. Wołoszyn J, Szopa K, Czerwiński G. Enhanced heat transfer in a PCM shell-and-tube thermal energy storage system. Appl Therm Eng. 2021;196:117332. https://doi.org/10.1016/j.applthermaleng.2021.117332.
27. Qaiser R, Khan MM, Khan LA, Irfan M. Melting performance enhancement of PCM based thermal energy storage system using multiple tubes and modified shell designs. J Energy Storage. 2021;33:102161. https://doi.org/10.1016/j.est.2020.102161.
28. Abderrahmane A, Qasem NA, Mourad A, Al-Khaleel M, Said Z, Guedri K, et al. Enhancing the melting process of shell-and-tube PCM thermal energy storage unit using modified tube design. Nanomaterials. 2022;12(17):3078. https://doi.org/10.3390/nano12173078.
29. Sardari PT, Mohammed HI, Giddings D, Gillott M, Grant D. Numerical study of a multiple-segment metal foam-PCM latent heat storage unit: effect of porosity, pore density and location of heat source. Energy. 2019;189:116108. https://doi.org/10.1016/j.energy.2019.116108.
30. Tiji ME, Mohammed HI, Ibrahem RK, Dulaimi A, Mahdi JM, Sh. Majdi H, et al. Evaluation of T-shaped fins with a novel layout for improved melting in a triple-tube heat storage system. Front Energy Res. 2022;10:947391. https://doi.org/10.3389/fenrg.2022.947391.
31. Sultan HS, Mohammed HI, Biswas N, Togun H, Ibrahem RK, Mahdi JM, et al. Revolutionizing the latent heat storage: boosting discharge performance with innovative undulated phase change material containers in a vertical shell-and-tube system. J Comput Des Eng. 2024;11(2):122–45. https://doi.org/10.1093/jcde/qwae020.
32. Sajadian S, Hosseinzadeh K, Akbari S, Rahbari A, Talebizadehsardari P, Keshmiri A. Discharge optimization in shell-and-tube latent heat storage systems using response surface methodology. Results Eng. 2025;25:104157. https://doi.org/10.1016/j.rineng.2025.104157.
33. Yang S, Zhang Y, Zhao Y, Torres JF, Wang X. PCM-based ceiling panels for passive cooling in buildings: a CFD modelling. Energy Build. 2023;285:112898. https://doi.org/10.1016/j.enbuild.2023.112898.
34. Öztop HF, Gür M, Selimefendigil F, Coşanay H. Impacts of inclined plate on melting time for phase change material filled blocks: experimental and numerical analysis. Therm Sci Eng Prog. 2024;48:102427. https://doi.org/10.1016/j.tsep.2024.102427.
35. Hammoodi KA, Alshukri MJ, Ibrahim OAAM, Kadhim SA, Nayyaf DR, Alsayah AM, et al. Influence of air velocity on enhancing heat transfer rate in phase change materials for efficient device temperature control. Heliyon. 2025. https://doi.org/10.1016/j.heliyon.2025.e43003.
36. Kumar M, Krishna DJ. Influence of mushy zone constant on thermohydraulics of a PCM. Energy Procedia. 2017;109:314–21. https://doi.org/10.1016/j.egypro.2017.03.074.
37. Khalaf AF, Rashid FL, Letif SA, Ameen A, Mohammed HI. A numerical study of the effect of water speed on the melting process of phase change materials inside a vertical cylindrical container. Appl Sci. 2024;14(8):3212. https://doi.org/10.3390/app14083212.
38. Hammoodi KA, Kadhim SA, Nayyaf DR, Hussein KKA, Mohammed ZI, Askar AH, et al. Investigation of the influence of the air layer on the phase change material melting process inside a hemicylindrical enclosure: a numerical approach. Results Eng. 2024;24:103337. https://doi.org/10.1016/j.rineng.2024.103337.
39. Esapour M, Hamzehnezhad A, Darzi AAR, Jourabian M. Melting and solidification of PCM embedded in porous metal foam in horizontal multi-tube heat storage system. Energy Convers Manage. 2018;171:398–410. https://doi.org/10.1016/j.enconman.2018.05.086.
40. Voller VR, Prakash C. A fixed grid numerical modelling methodology for convection-diffusion mushy region phase-change problems. Int J Heat Mass Transfer. 1987;30(8):1709–19. https://doi.org/10.1016/0017-9310(87)90317-6.
41. Brent AD, Voller VR, Reid KTJ. Enthalpy-porosity technique for modeling convection-diffusion phase change: application to the melting of a pure metal. Numer Heat Transf A Appl. 1988;13(3):297–318. https://doi.org/10.1080/10407788808913615.
42. Kadhim SA, Askar AH, Saleh AAM. An enhancement of double pipe heat exchanger performance at a constant wall temperature using a nanofluid of iron oxide and refrigerant vapor. J Therm Eng. 2024;10(1):78–87. https://doi.org/10.18186/thermal.1429191.
43. Al-Yasiri Q, Szabó M. Hourly analysis of temperature and heat gain reduction for building envelope-compacted phase change material in extremely hot conditions. J Energy Storage. 2023;68:107838. https://doi.org/10.1016/j.est.2023.107838.
44. Hosseini MJ, Ranjbar AA, Sedighi K, Rahimi M. A combined experimental and computational study on the melting behavior of a medium temperature phase change storage material inside shell and tube heat exchanger. Int Commun Heat Mass Transfer. 2012;39(9):1416–24. https://doi.org/10.1016/j.icheatmasstransfer.2012.07.028.
45. Kadhim SA, Ibrahim OAAM. The effect of holes number in cylindrical samples on the forced convection heat flow. Int J Mech Eng Robot Res. 2022;11(6):429–36. https://doi.org/10.18178/ijmerr.11.6.429-436.

Publisher's Note

Springer Nature remains neutral with regard to jurisdictional claims in published maps and institutional affiliations.